GLOBAL PHOTOMETRY OF ASTEROID (101955) BENNU WITH OVIRS. X.-D. Zou[1], J.-Y. Li[1], B. E. Clark[2], D. R. Golish[3], H. H. Kaplan[4], V. E. Hamilton[4], A. A. Simon[5], D. C. Reuter[5], E. S. Howell[3], S. Ferrone[3], J. P. Emery[6], D. N. DellaGiustina[3], C. W. Hergenrother[3], M. A. Barucci[7], S. Fornasier[7], P. H. Hasselmann[7], C. A. Bennett[3], M. C. Nolan[3], O. S. Barnouin[8], D. S. Lauretta[3], [1]Planetary Science Institute, 1700 E Fort Lowell Rd, Ste 106, Tucson, AZ, 85719, USA (zouxd@psi.edu, jyli@psi.edu), [2]Ithaca College, Ithaca, NY, USA, [3]Lunar and Planetary Laboratory, University of Arizona, Tucson, AZ, USA, [4]Southwest Research Institute, Boulder, CO, USA, [5]Goddard Space Flight Center, Greenbelt, MD, USA, [6]Northern Arizona University, Flagstaff, AZ, USA, [7]LESIA, Observatoire de Paris-Meudon, France, [8]Johns Hopkins University Applied Physics Laboratory, Laurel, MD, USA.

Introduction: The primary objective of NASA's OSIRIS-REx mission [1] is to return a sample of asteroid (101955) Bennu to Earth. Results from OSIRIS-REx show Bennu is hydrated and volatile-rich [2], but with a far rockier than predicted surface. Images from OCAMS [3], revealed distinct albedo and color variations on Bennu surface [4]. We investigate the global photometric properties of Bennu as observed by the OSIRIS-REx Visible and InfraRed Spectrometer (OVIRS) [5] from December 9 2018 to June 6 2019. The aim of this work is to characterize global averaged disk-resolved photometric properties with multiple photometric models. The analyses are performed over wavelengths ranging from 0.39 to 3.7 microns and phase angle ranging from 5.28 to 132.62 degrees. We modeled the surface of Bennu with five empirical models and a simplified Hapke model. The pipeline best-fit Minnaert model was applied to correct the observation of Bennu to standard observation geometry at VIS-IR wavelength. We also derived the bolometric Bond albedo map of Bennu. The phase reddening effect and surface properties are also analyzed and compared to other asteroids. The surface composition discoveries using OVIRS data are discussed in other reports in this same conference [6-9].

Dataset: In this study, we analyze data from the Preliminary Survey (PS), Detailed Survey–Baseball Diamond (BBD) and Detailed Survey–Equatorial Stations (EQ) mission phases [1]. The light-scattering geometry angles (I, incidence angle; e, emission angle; and α, phase angle) used for photometric modeling are derived by the mission's automatic pipeline. It derived the incidence and emission angles by averaging the vectors of 100 rays in each light cone of the OVIRS observation geometry using the stereophotoclinometry (SPC) shape model v20 [10]. The ground calibration pipeline converts the raw data (counts/second) to physical units (W/cm2/sr/micron) and then to spot I/F (radiance factor, RADF). The performance of OVIRS was validated with Earth flyby data [11].

Global disk resolved photometry:

Data reduction. To investigate the global photometric properties, we need to select the spots to form the input dataset for photometry. We follow the steps to construct the dataset for photometric modeling: 1) Select only OVIRS spots that contain the illuminated portion of the asteroid, filling the field of view. 2) Filter out spots with incidence or emission angles greater than 70°. 3) Exclude all the spectra with large noise (>1.2 mean value) or negative value due to saturation based on filtering the 0.39–3.7 μm parts. 4) Exclude spots from off-nominal observation.

Fitting with empirical models. Our photometry pipeline was intended to be automated for the rapid analysis of OVIRS data for decision-making on tactical timescales. It was built in the pre-encounter phase of mission with the Lommel-Seeliger, Minnaert, McEwen, Linear-Akimov, and Akimov models.

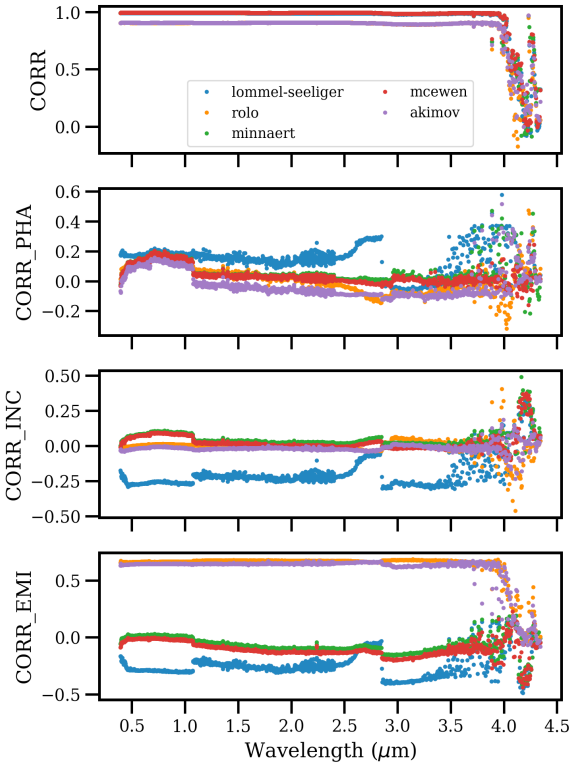

Fig. 1. Model correlation ratio (top) and correlation ratio against geometry angles (phase, incidence and emission).

We evaluate the pipeline fitting quality using correlation (Fig. 1) and slope calculations. These quality plots show similar results; the Minnaert and McEwen

models overall are better quality. Two Akimov models have strong bias with respect to emission angles. The L-S model has strong bias against all three angles. The segment boundaries are clearly apparent in the quality plot for all models.

Photometric correction. The OVIRS spectral reflectance of Bennu's surface depends on the light scattering geometry. In order to make comparisons between different areas and quantitatively interpret the spectra based on laboratory measurements, the observations need to be photometrically corrected to the same geometry. In our pipeline we use a common geometry often used in laboratory setting, (i0, e0, α0) = (30°, 0°, 30°) as our default reference angles. The pipeline best-fit Minnaert model is used to correct all the RADF values of each spectral band to the reference angle. Before correction, a smoothing procedure (a one dimension and 51 length boxcar filter with polynomial order three on each non-scaling parameter) is applied on the model parameters over the wavelengths ranging from 0.4 to 3.7 μm to reduce the noise of each band caused by ignoring the fact that the bands are not independent when we model them separately.

Hapke modeling. We adopted a five-parameter form of Hapke model [12, 13] and fixed two parameters as $b0 = 1$ and $h = 0.01$. We compare the photometric properties with w (SSA, Single Scattering Albedo), g, and θ. The global average Hapke modeling results are shown in Fig. 2. And we will report the analyses for the physical properties base on this modeling.

Photometric uncertainty. We measure the uncertainty of the photometric correction in terms of how much the photometric correction changed the spectrum result in 6%. When we make a phase ratio we expect a generally low frequency gentle wavelength dependence, such as a slope. We also expect that inside of absorption features we will see a sharper wavelength dependence to the phase ratio. Based on this assumption we measured the uncertainty with model phase ratio as 6% also.

Further analyses:

Phase reddening effect and compare to other asteroids. Here we will present the phase reddening observation with OVIRS and the compare of the results to other asteroids.

Acknowledgments:

This material is based upon work supported by NASA under Contract NNM10AA11C issued through the New Frontiers Program. We are grateful to the entire OSIRIS-REx Team for making the encounter with Bennu possible.

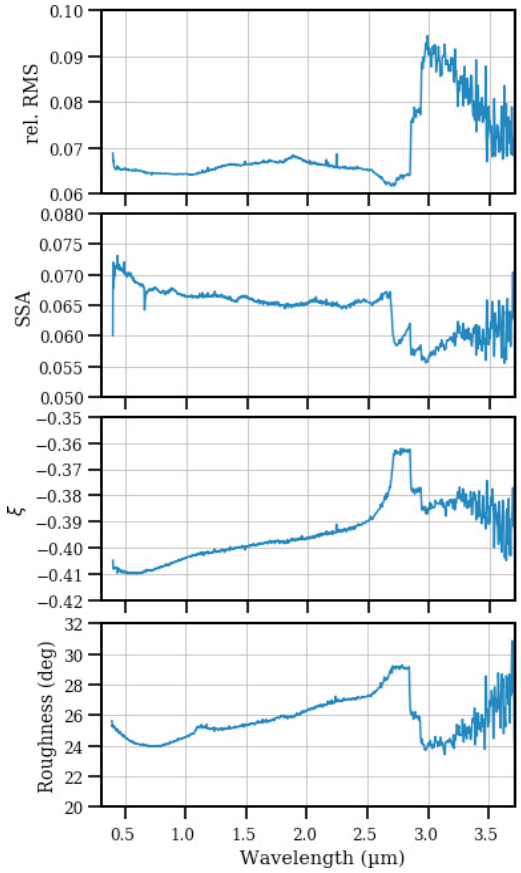

Fig. 2. Global Hapke modeling result.

References: [1] Lauretta D.S. et al. (2017) *Space Sci. Rev.*, *212,* 925-984. [2] Hamilton V.E. et al. (2019). *Nat. Astron,*. *3,* 332–340.[3] Rizk B. et al. (2018) *Space Sci. Rev., 214,* 26.[4] DellaGiustina D.N. & Emery J.P. et al. (2019) *Nat. Astron., 3,* 341–351.[5] Reuter D.C. et al. (2018) *Space Sci. Rev., 214*, 54. [9] Simon A. A. (2020) *LPS LI,* Abstract #1046. [10] Hamilton E. V. (2020) *LPS LI,* Abstract #1049. [11] Kaplan H. H. (2020) *LPS LI,* Abstract #1050. [12] Praet A. (2020) *LPS VII,* Abstract #1058. [10] Barnouin O.S. et al. (2019) *Nat. Geosci., 12,* 247–252.[11] Simon A.A. et al. (2018) *Remote Sens., 10*, 1486. [12] Hapke B. (2012) *Cambridge university press.* [13]Li et a. (2009) Icarus, 204, 209-226.